Visualization of mycobacterial membrane dynamics in live cells

Frances P. Rodriguez-Rivera,[†,‡] Xiaoxue Zhou,[§] Julie A. Theriot,[§,∥,#] and Carolyn R. Bertozzi*[,‡,#]

[†]Department of Chemistry, University of California, Berkeley, California 94720, United States

[‡]Department of Chemistry, Stanford University, Stanford, California 94305, United States

[§]Department of Biochemistry and [∥]Department of Microbiology and Immunology, Stanford University School of Medicine, Stanford, California 94305, United States

[#]Howard Hughes Medical Institute, Chevy Chase, Maryland 20815, United States

Ⓢ Supporting Information
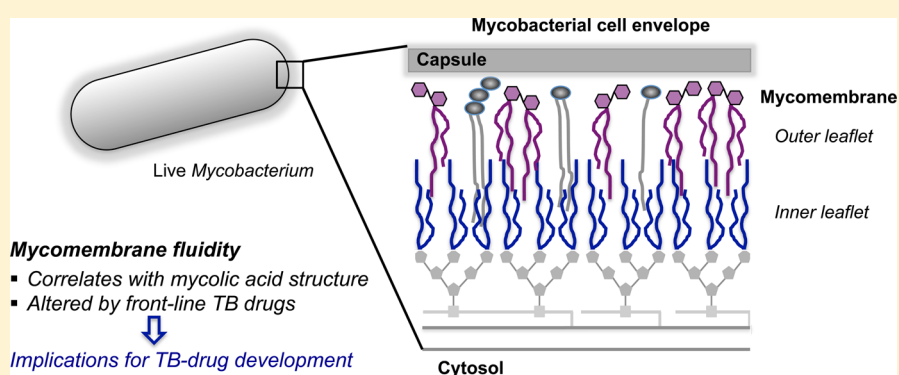
ABSTRACT: Mycobacteria are endowed with a highly impermeable mycomembrane that confers intrinsic resistance to many antibiotics. Several unique mycomembrane glycolipids have been isolated and structurally characterized, but the underlying organization and dynamics of glycolipids within the cell envelope remain poorly understood. We report here a study of mycomembrane dynamics that was enabled by trehalose−fluorophore conjugates capable of labeling trehalose glycolipids in live actinomycetes. We identified fluorescein−trehalose analogues that are metabolically incorporated into the trehalose mycolates of representative *Mycobacterium*, *Corynebacterium*, *Nocardia*, and *Rhodococcus* species. Using these probes, we studied the mobilities of labeled glycolipids by time-lapse microscopy and fluorescence recovery after photobleaching experiments and found that mycomembrane fluidity varies widely across species and correlates with mycolic acid structure. Finally, we discovered that treatment of mycobacteria with ethambutol, a front-line tuberculosis (TB) drug, significantly increases mycomembrane fluidity. These findings enhance our understanding of mycobacterial cell envelope structure and dynamics and have implications for development of TB drug cocktails.

■ INTRODUCTION

Tuberculosis (TB), the leading cause of death worldwide from a single infectious agent, *Mycobacterium tuberculosis* (*Mtb*), took 1.5 million lives in 2014 and remains a global public health emergency.[1] *Mtb* infects host macrophages, and survival within that hostile environment depends on an impermeable cell envelope that protects bacilli from biological stresses.[2,3] Furthermore, the cell envelope has proven to be a formidable physical barrier against many antibiotics that might otherwise be efficacious against *Mtb*.[4,5] For this reason, TB must be treated with drug combinations that include at least one compound that compromises cell envelope integrity.[6]
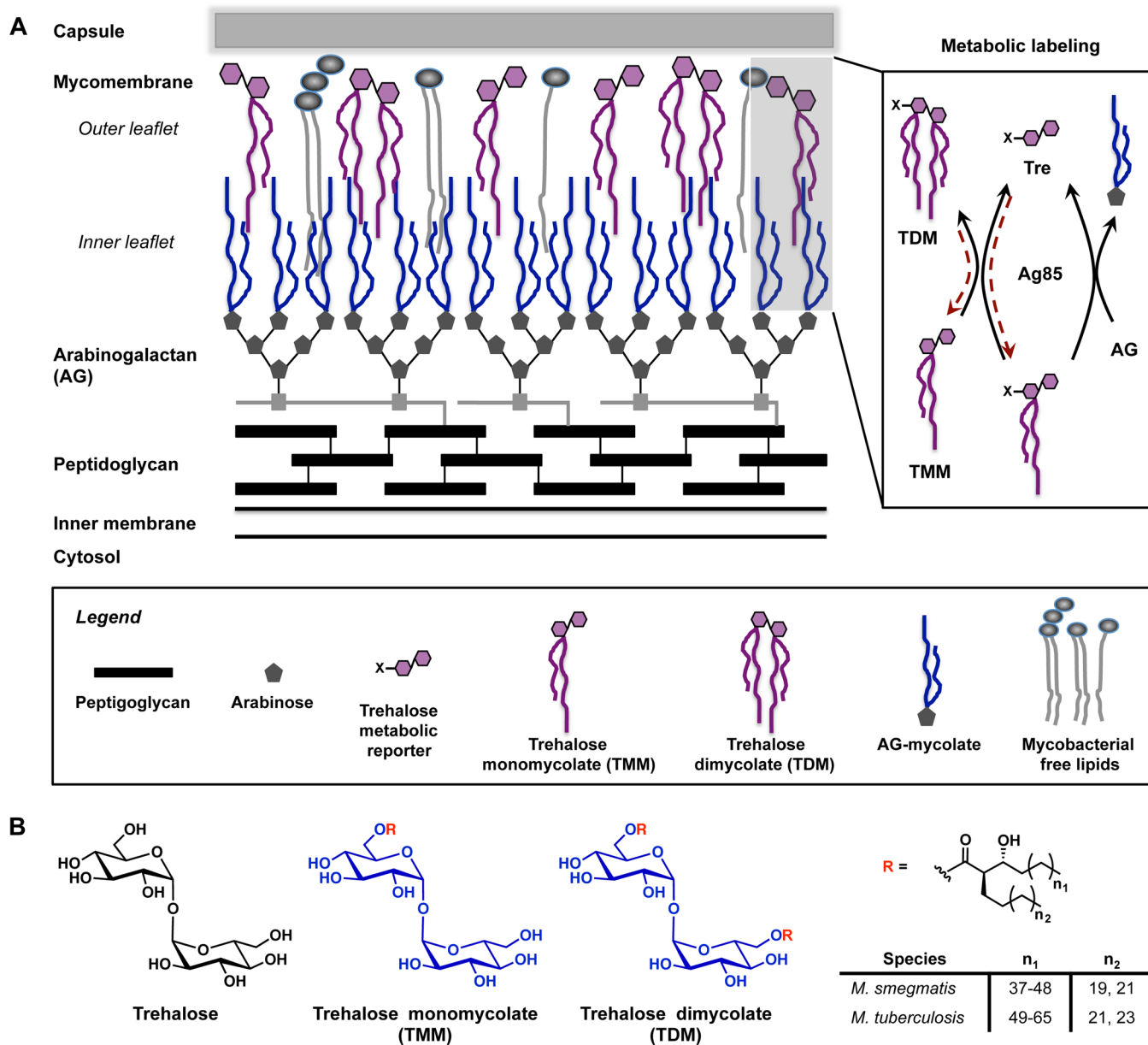
The mycobacterial cell envelope comprises inner membrane and peptidoglycan layers that are similar to those of common Gram-negative and Gram-positive organisms but then diverges considerably in the molecular composition of its outer layers (Figure. 1A). Most prominent are mycolic acids that are covalently anchored to arabinogalactan chains.[7] Up to an impressive 90 carbon atoms in length,[8] these lipids constitute the inner leaflet of the mycomembrane and form an interface with an outer leaflet composed of noncovalently associated glycolipids, the most abundant being trehalose monomycolate (TMM) and dimycolate (TDM) (Figure 1B). The result is a functional outer membrane that is unique to *Mtb* and other members of the suborder *Corynebacterinae*.

Given its importance in protecting *Mtb* from drug action, the cell envelope has been a focus of considerable structural work centered on isolating and identifying its various components and visualizing layers by electron microscopy (EM).[7] CryoEM studies have added information about the highly organized vertical architecture of the cell envelope at high resolution and in a native state.[9,10] Far less is known, however, about the dynamics of the cell envelope, and very few studies have

Figure 1. Mycobacterial cell envelope and structures of trehalose mycolates. (A) Mycobacterial cell envelope components include inner membrane, peptidoglycan, arabinogalactan, mycomembrane, and capsule. Antigen 85 mediates mycolylation of arabinogalactan from TMM donor. Two molecules of TMM are used to generate TDM, thereby releasing one molecule of trehalose. Antigen 85 is predicted to be active in the mycomembrane. Red dashed line depicts metabolic incorporation route for unnatural trehalose reporters. (B) Chemical structures for trehalose, trehalose monomycolate, and trehalose dimycolate. Number of carbons (n_1, n_2) strictly in linear chains of mycolates are shown for *M. smegmatis* and *M. tuberculosis*. Trehalose (Tre), antigen 85 (Ag85), arabinogalactan (AG).

focused on the mycomembrane, the major contributor to barrier function. This deficit likely reflects a lack of tools for probing cell envelope metabolites in live cells, and with subcellular resolution, a problem that chemists have tackled in recent years with the development of new imaging methods.[11] For example, early work using lipophilic fluorophore conjugates that nonspecifically intercalate into the mycomembrane suggested a heterogeneous cell surface landscape.[12,13] Progress toward defining the dynamic properties of *Mtb*'s cell envelope, however, requires more refined methods for imaging its specific cell envelope components.

Recently, metabolic labeling has proven to be an effective strategy to image trehalose glycolipids in the mycomembrane of live mycobacteria.[14−17] The approach exploits the promiscuity of the antigen 85 complex (Ag85), a family of mycolyl-transferases that convert two molecules of TMM to TDM and free trehalose (Figure 1A). In a screen of dozens of trehalose analogues, Backus et al. found that the backward reaction can be used to deliver unnatural trehalose derivatives into *Mtb*'s mycomembrane (Figure 1A), including a fluorescein conjugate (FITC-Tre, Figure 2A).[14] This observation suggests a means by which mycomembrane dynamics could be directly interrogated by molecular imaging.

Here, we identified fluorescein−trehalose analogues that are recognized by mycolyltransferases of diverse actinobacterial species, including *Mycobacteria*, *Corynebacteria*, *Nocardia*, and *Rhodococcus* genera. We used the new probes to determine the subcellular distribution and dynamics of trehalose mycolates
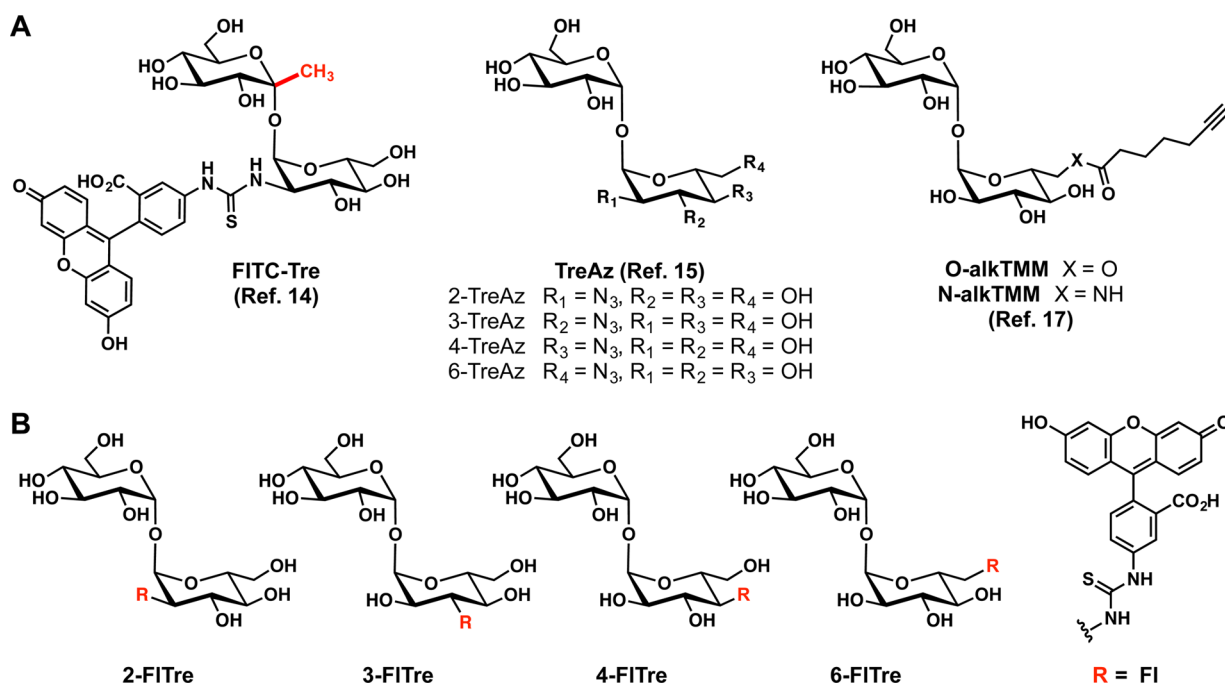
Figure 2. Metabolic engineering of trehalose glycolipids with unnatural trehalose reporters. (A) Previously reported unnatural trehalose reporters including FITC-Tre, TreAz analogues, and alkTMM analogues. (B) Library of fluorescein−trehalose analogues (this work). Fluorescein isothiocyanate (FITC), azido−trehalose (TreAz), fluorescein−trehalose (FlTre).

within the mycomembrane of live cells. Using fluorescence recovery after photobleaching (FRAP) experiments, we found a striking disparity in mycomembrane mobilities across species, which partially correlated with mycolic acid structure. Finally, we probed the effects of the front-line TB drug ethambutol on mycomembrane dynamics in live *M. smegmatis* cells. We conclude that drugs targeting the *Mtb* cell envelope influence mycomembrane fluidity, and this parameter might therefore be considered when evaluating new drug combinations.

■ RESULTS AND DISCUSSION

Design and Synthesis of New Fluorescein−Trehalose Conjugates. Our first goal was to develop a fluorescent trehalose reagent that efficiently labels trehalose mycolates across many actinobacterial species. A survey of previously reported trehalose analogues revealed them to be unsuitable for various reasons. We found that FITC-Tre (Figure 2A) labeled *Mycobacteria* and *Nocardia* species with poor efficiency and did not label glycolipids of *Corynebacteria* at a detectable level (*vide infra*). We speculate that the anomeric methyl group (highlighted in red, Figure 2A), a directing group used by Backus et al. to form the α,α-1,1-glycosidic linkage, may compromise the processing of FITC-Tre by the Ag85 complex.[14]

Alternatively, we considered our own previously reported azido−trehalose derivatives (TreAz, Figure 2A), which are metabolically incorporated into trehalose glycolipids by several mycobacterial species and through both cytosolic and extracellular pathways.[15] However, these analogues get transformed to additional classes of trehalose metabolites beyond TMM and TDM, which complicates data interpretation. Moreover, the secondary reagents used to attach fluorescent probes (e.g., cyclooctyne−fluorophore conjugates) have limited access to the mycomembrane and engage in nonspecific interactions. Recently, Swarts and co-workers elegantly

introduced alkyne-functionalized trehalose analogues (alkTMM, Figure 2A) into the mycomembrane.[17] This approach also requires the use of secondary labeling reagents as well as Cu catalyst that may be cytotoxic.

In light of these issues, we returned to the notion of one-step labeling with a trehalose−fluorophore conjugate and focused on developing reagents with improved metabolic efficiency compared to FITC-Tre. Accordingly, we synthesized the panel of regioisomeric fluorescein−trehalose conjugates (FlTre, shown in Figure 2B), which all possess a native trehalose core structure. The compounds were prepared from the corresponding TreAz analogues by reduction to the amines followed by reaction with fluorescein isothiocyanate (FITC) (details provided in Supporting Information). Notably, 2-, 3-, and 4-FlTre could, if recognized by Ag85, label both TMM and TDM, whereas 6-FlTre can only be metabolized to TMM.

Fluorescein−Trehalose Analogues Selectively Label Trehalose Mycolates. We tested the labeling activity of the FlTre analogues as well as FITC-Tre using live cultures of *Mycobacterium smegmatis* and *Corynebacterium glutamicum*, organisms whose cell envelope composition and structure are similar to those of *Mtb*.[18] All FlTre analogues outperformed FITC-Tre in both species as evaluated by flow cytometry (Figure 3A,B). Surprisingly, FITC-Tre was not metabolized at a detectable level by *C. glutamicum*, while 2-FlTre, which only differs from FITC-Tre by lacking an anomeric methyl group, was labeled strongly (Figure 3B). This observation illustrates that small perturbations to probe structure can alter or, in this case, completely ablate labeling. The brightest labeling was observed with 6-FlTre, while 2-, 3-, and 4-FlTre showed lower labeling in both species.

In addition, we evaluated the spatial distribution of the fluorescence labeling by microscopy. Gratifyingly, cell envelope labeling was observed for both *M. smegmatis* and *C. glutamicum* after incubation with 100 μM FlTre for several doubling times
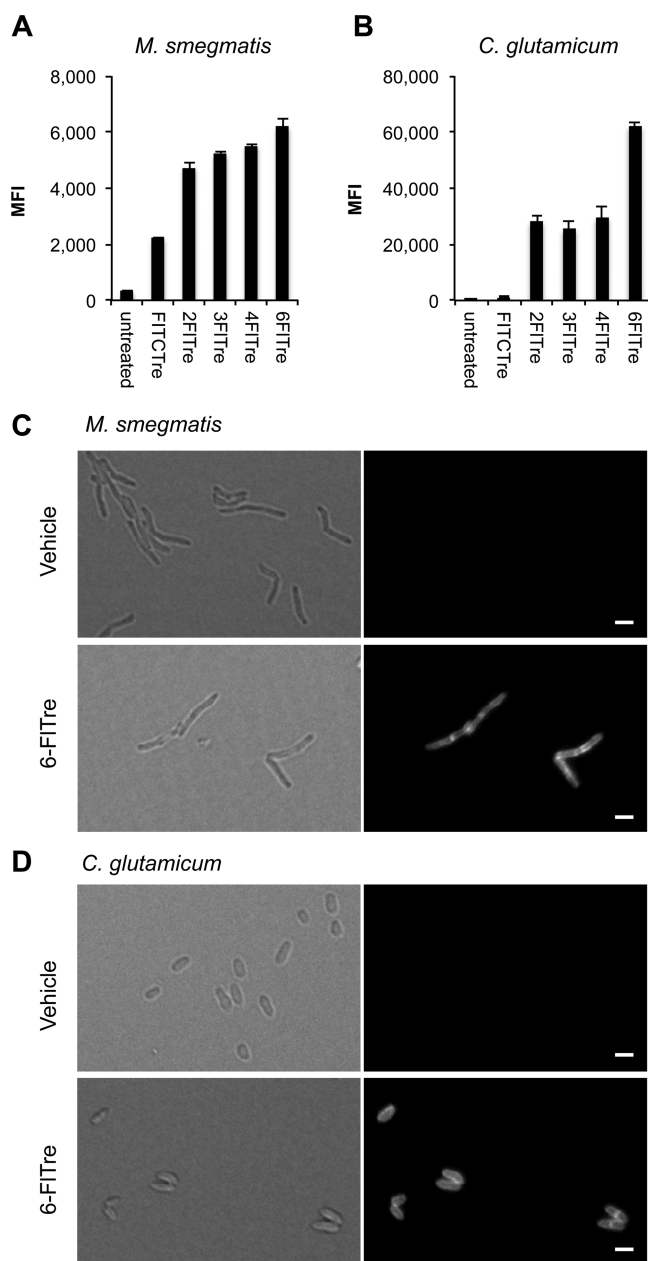
Figure 3. Metabolic labeling of actinobacteria with FlTre analogues. Labeling profile of FlTre analogues compared to FITC-Tre in *M. smegmatis* (A) and *C. glutamicum* (B). Bacteria were labeled with 100 μM trehalose analogues or vehicle for at least five doubling times and analyzed by flow cytometry. Error bars depict standard deviation of three replicate experiments. Results are representative of at least two independent experiments. Mean fluorescence intensity (MFI). Fluorescence microscopy images of *M. smegmatis* (C) and *C. glutamicum* (D) cells labeled with vehicle or 6-FlTre. Scale bar, 2 μm.

(Figure 3C,D, respectively). No defects in cell morphology were observed under these conditions. In particular, *M. smegmatis* showed polar labeling when treated for shorter incubations, suggesting incorporation into newly synthesized cell envelope, where biosynthetic enzymes reside[19,20] (Figure S1A). Treatment of bacteria that lack trehalose mycolates, such as canonical Gram-negative *Escherichia coli* and Gram-positive *Bacillus subtilis*, with 6-FlTre afforded no detectable labeling (Figure S1B).

To confirm that the FlTre isomers are biosynthetically converted to trehalose mycolates, we assessed whether exogenous trehalose, a native substrate for mycolyltransferases, could compete with reporter labeling. Bacterial cells that were co-incubated with 2-, 3-, 4-, or 6-FlTre (100 μM) and trehalose (0, 0.5, 5 mM) showed a dose-dependent decrease in metabolic labeling (Figure S2). In addition, we found that ebselen, an inhibitor of Ag85 activity in mycobacteria,[21,22] decreased 2-, 3-, 4-, and 6-FlTre labeling in both *M. smegmatis* and *C. glutamicum* (Figure S2). Furthermore, partially purified trehalose glycolipids from 2- or 6-FlTre-labeled *C. glutamicum* were analyzed by mass spectrometry. For both analogues, we observed ions corresponding to the expected fluorescein-conjugated TMM analogues (Figure S3 and Table S1). Finally, total lipids extracted from 6-FlTre-labeled *M. smegmatis* cells showed a single fluorescent band by thin-layer chromatography (Figure S3). Collectively, these data demonstrate that FlTre analogues are biosynthetically converted to trehalose mycolates in live bacterial cells.

Fluorescein−Trehalose Analogues Report on Mycomembrane Dynamics in Live Bacteria. We next sought to investigate the mobility of trehalose glycolipids in the mycomembrane during the course of cell growth. To that end, we performed two-color imaging experiments wherein we first labeled cells with 6-FlTre to visualize trehalose glycolipids, then later marked the newly formed cell wall with a peptidoglycan (PG) reporter, tetramethylrhodamine D-lysine (TDL), which replaces D-alanine residues in the stem peptides.[23] *M. smegmatis* was labeled with 6-FlTre for several generations, washed to remove excess reporter, and chased with TDL for 5 or 20 min (Figure 4A). Fluorescence microscopy revealed that labeled trehalose mycolates were excluded from newly biosynthesized cell wall at the poles during growth, as denoted by minimal overlap with polar labeling of PG. These results suggest that trehalose glycolipids in the mycomembrane remain rather immobile during growth in *M. smegmatis*. Conversely, *C. glutamicum* showed complete redistribution of labeled glycolipids after 6-FlTre had been removed from the growth media for the same time periods (Figure 4B). We were intrigued by the lack of fluidity in the mycobacterial mycomembrane that did not allow diffusion of labeled trehalose glycolipids to new cell envelope regions. Indeed, low fluidity has been predicted based on extremely low permeability of the mycomembrane to lipophilic molecules[24] as well as differential scanning calorimetry (DSC) studies that revealed high-temperature phase transitions in *Mycobacteria*.[25−27] Our results provide direct experimental confirmation of this prediction in live cells.
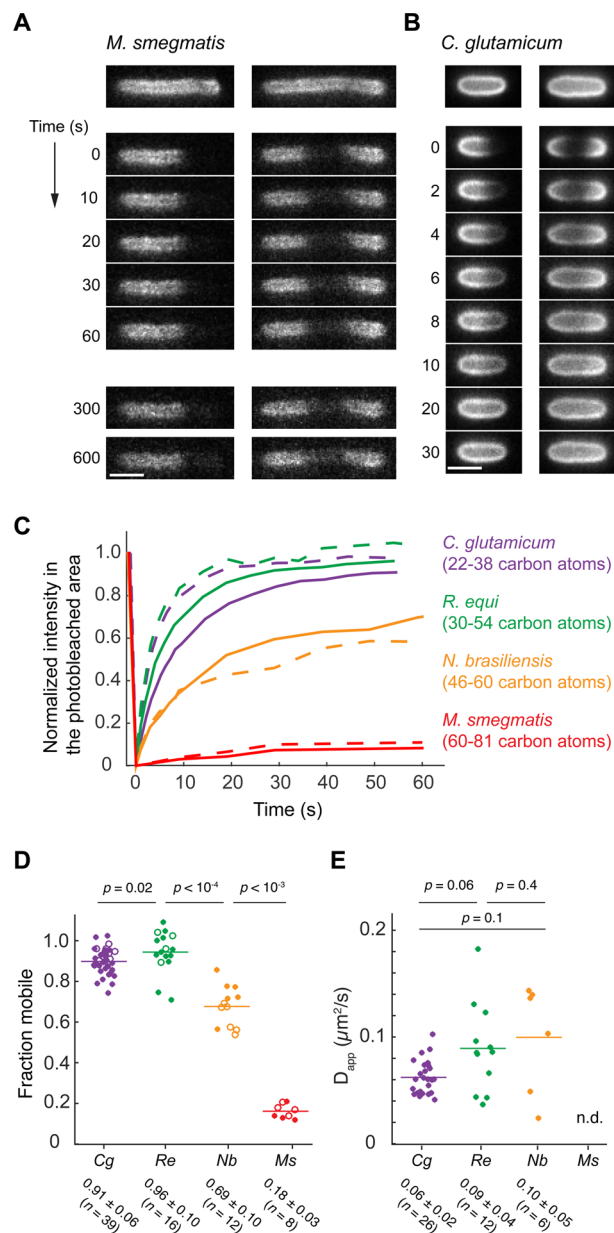
Mycolic-Acid-Producing Actinobacteria Have a Wide Range of Mycomembrane Fluidities That Correlate with Mycolic Acid Chain Structure. Fluorescence recovery after photobleaching (FRAP)[28] experiments have been previously used to quantitate diffusion dynamics and subcellular organization of membrane components in live bacteria with high temporal and spatial resolution.[29] We therefore applied the FRAP technique to directly elucidate the intrinsic mobility of labeled trehalose glycolipids in mycobacteria. Photobleaching of polar and midcellular regions of *M. smegmatis* prelabeled with 6-FlTre revealed that trehalose glycolipids failed to move after irradiation (Figure 5A), even when monitored up to 10 min. However, under the same experimental conditions, *C. glutamicum* glycolipids diffused through the photobleached area in a few seconds (Figure 5B). The relatively high fluidity
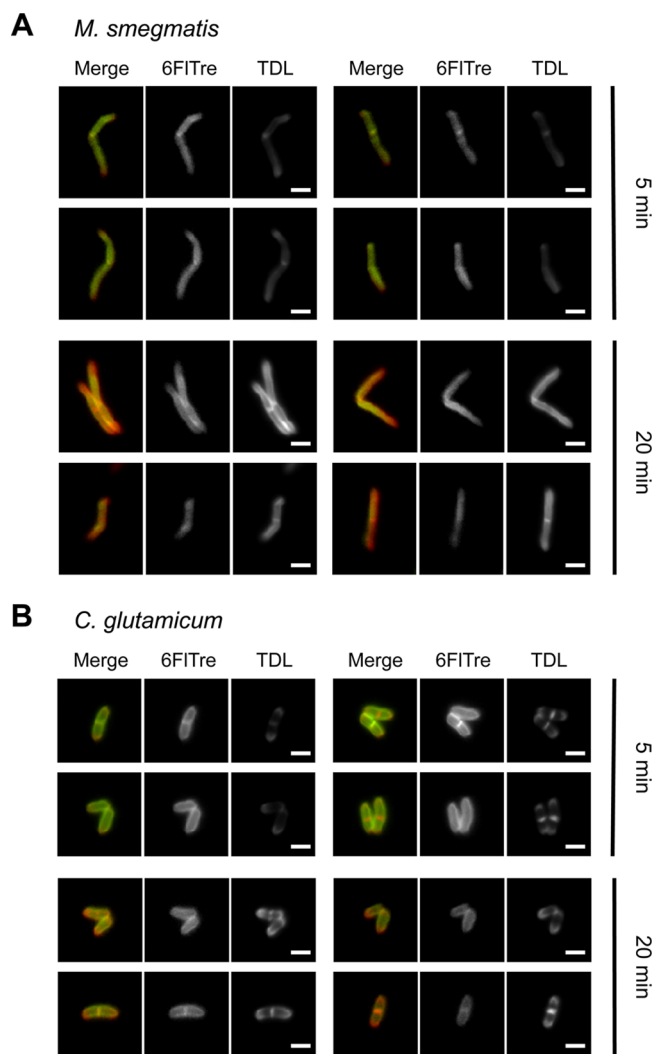
Figure 4. FlTre-labeled trehalose glycolipids show species-dependent mobility. (A) Prelabeled *M. smegmatis* glycolipids (6-FlTre, green) are excluded from the poles as depicted by peptidoglycan labeling (TDL, red). (B) Prelabeled *C. glutamicum* glycolipids are highly mobile and redistribute to the entire cell after 6-FlTre is removed from the growth media. Scale bar, 2 μm.

Figure 5. Mycobacterial trehalose glycolipids are relatively immobile. FRAP experiment of 6-FlTre labeled *M. smegmatis* (A) and *C. glutamicum* (B) after irradiation at the pole (left panel) and center (right panel). Scale bar, 2 μm. (C) Fluorescence recovery curves after photobleaching for center and pole regions in 6-FlTre-labeled cells across different bacterial species with the corresponding number of carbon atoms in mycolic acid chains. Lines represent the averaged signal of $n \geq 6$ cells, where solid and dotted lines correspond to pole and center regions, respectively. Comparison of fraction mobile (D) and apparent diffusion coefficient (E) extracted from fitting FRAP curves for different actinobacterial species. Filled and open circles correspond to pole and center regions, respectively. Number of cells evaluated with the corresponding mean and standard deviation are shown for every species; p values between samples were calculated with a rank sum test. *M. smegmatis* (Ms), *C. glutamicum* (Cg), *R. equi* (Re), *N. brasiliensis* (Nb), apparent diffusion coefficient (D_{app}), not determined (nd).

observed for the corynebacterial mycomembrane is consistent with previously reported lower-temperature phase transitions as measured by DSC.[25] Quantitation of fluorescence recovery traces and half-time measurements revealed similar recovery dynamics regardless of the photobleached area of the cell (pole or center), as shown in Figure 5C. Similar glycolipid mobility phenomena were also observed when cells were labeled with 2-FlTre (Figure S5) or trehalose reporters modified with different fluorophores at the same position (Figure S6; probe characterization is shown in Figure S4), suggesting that the glycolipid dynamics we observed are not significantly altered by probe structure. In addition, for a control experiment, we performed FRAP analysis on cells that were metabolically labeled with D-amino acid reporters bearing the same fluorophores. As expected, the fluorophores integrated into PG were essentially immobile (Figure S7).

In order to get a more quantitative understanding of observed diffusion phenomena, we modeled recovery data to calculate the apparent diffusion coefficients for labeled trehalose mycolates (Figure S8). A diffusion coefficient of 0.06 ± 0.02

μm² s⁻¹ ($n = 20$ cells) was obtained for 6-FlTre-labeled glycolipids in *C. glutamicum*, while the lack of observable diffusion in *M. smegmatis* limited our ability to model fluorescence recovery. For comparison, lipopolysaccharide
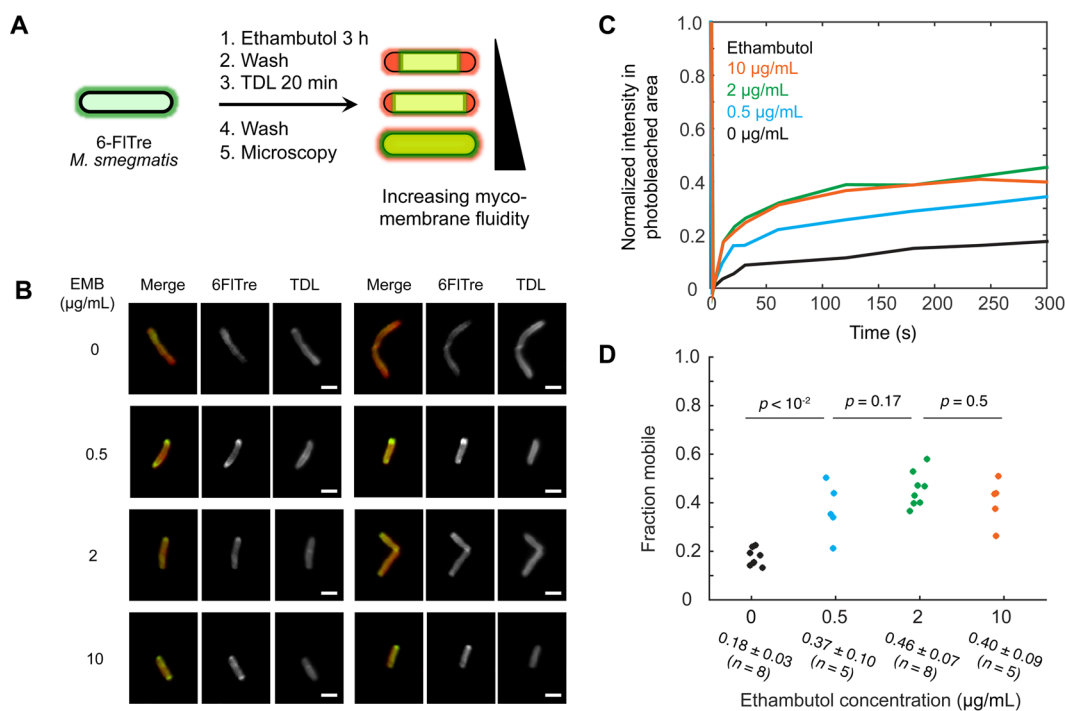
Figure 6. FlTre metabolic labeling reports on cell envelope dynamics during ethambutol (EMB) treatment. (A) Scheme depicting experimental workflow and labeling pattern expected for differential mycomembrane fluidity. *M. smegmatis* was prelabeled with 6-FlTre and then treated with EMB at different concentrations for 3 h. Cells were washed to remove excess 6-FlTre and chased with TDL in the absence of drug for 20 min. (B) Spatial distribution of labeled glycolipids was evaluated by fluorescence microscopy after fixation. Representative cells are shown in each panel. 6-FlTre and TDL signals are in green and red channels, respectively, for merged images (left panel). FRAP recovery traces (C) and fraction mobile (D) for cells treated with different concentrations of EMB. Fluorescence recovery trace lines represent the averaged signal of $n \geq 5$ cells. Number of cells evaluated with the corresponding mean and standard deviation are shown for all concentrations; *p* values between samples were calculated with a rank sum test. Scale bar, 2 μm.

(LPS), an abundant glycolipid in the outer membrane of Gram-negative *E. coli*, diffuses slightly slower ($0.020 \pm 0.009 \ \mu m^2 \ s^{-1}$) as determined by an exogenous rhodamine−LPS conjugate.[30] However, antibody binding of LPS to visualize glycolipid dynamics resulted in much slower diffusion dynamics ($2.0 \times 10^{-5} \ \mu m^2 \ s^{-1}$),[31] suggesting potential perturbation by antibody detection and underscoring the benefits of directly visualizable glycolipids.

Our results, consistent with DSC studies, suggest a potential correlation between trehalose mycolate structure and the empirically determined fluidity of the mycomembrane. Mycolic acid chain lengths vary significantly between *C. glutamicum* (22−38 carbon atoms)[32] and *M. smegmatis* (60−81 carbon atoms).[33] Fascinated by the dramatic differences in trehalose glycolipid mobility observed for *M. smegmatis* and *C. glutamicum*, we sought to test the correlation of mycomembrane fluidity and mycolic acid length by extending our analysis to other bacterial species. *Rhodococcus* and *Nocardia* species synthesize trehalose glycolipids with intermediate length mycolic acids, ranging from 30 to 54 and 46 to 60 carbon atoms, respectively.[34,35] We thus hypothesized that *Rhodococcus equi* and *Nocardia brasiliensis* would show intermediate glycolipid mobilities relative to corynebacteria and mycobacteria. FlTre analogues labeled both species as confirmed by flow cytometry and fluorescence microscopy (Figure S9). FRAP mobility studies revealed similar fluorescence recovery profiles for *R. equi* and *C. glutamicum*, whereas *N. brasiliensis* displayed an intermediate recovery profile (Figure 5C). These results were corroborated by evaluation of the fraction mobile of labeled trehalose glycolipids, which showed striking differences

between all bacterial species (Figure 5D). Calculated apparent diffusion coefficients revealed small differences between species that were not statistically significant, suggesting subtle effects on diffusion for minor variations in mycolic acid chain length. The diffusion coefficient for *M. smegmatis* was not calculated because recovery was not observed after 10 min (Figure 5A). However, functional groups such as ketones, methoxy, and cyclopropyl groups in mycobacterial mycolic acids significantly influence membrane fluidity as determined by DSC studies.[25−27,36] Taken together, our results correlate real-time mycomembrane fluidity to mycolic acid structure across several actinobacteria.

Ethambutol Treatment Alters Mycomembrane Dynamics. Impermeable membranes within the cell envelope can serve as static barriers against antibiotics and biological stresses. Genes involved in the biosynthesis of the bacterial cell envelope are essential for growth and division and thus are important antibiotic targets.[7,37] Our imaging strategy could find broad applications in characterizing mycobacterial cell wall changes in live cells upon treatment with current front-line TB drugs. For example, ethambutol inhibits arabinosyl transferase EmbB that installs arabinose residues to growing arabinogalactan chains,[38,39] which results in reduced sites for mycolylation of the inner leaflet of the mycomembrane. We hypothesized that the fluidity of the mycomembrane could be altered by treatment with ethambutol as a result of changing the membrane's physical properties.

We evaluated trehalose mycolate's mobility in 6-FlTre-prelabeled mycobacteria after ethambutol treatment. TDL labeling of PG marked cell wall biogenesis and also reported

on relative growth rates, an indicator of drug toxicity. *M. smegmatis* cells were prelabeled with 6-FlTre over several generations and treated with different ethambutol doses for 3 h while the reporter was still present. Cells were then chased with TDL for 20 min, washed, fixed, and imaged by microscopy. As shown in Figure 6A, untreated cells showed exclusion of prelabeled glycolipids from new cell wall regions. However, ethambutol treatment at doses as low as 0.5 μg/mL led to redistribution of labeled trehalose mycolates across the entire cell surface, with accumulation of signal at the poles (Figure 6B). *M. smegmatis* has been reported to upregulate trehalose mycolate biosynthesis after exposure to ethambutol,[40,41] which is consistent with higher metabolic labeling observed at the poles during drug treatment. Overall, these results indicate that ethambutol treatment enhances mycomembrane fluidity. Notably, we observed increased diffusion for subminimal inhibitory concentration (MIC) doses (ethambutol's MIC = 1.0 μg/mL for *M. smegmatis*[42]). To confirm ethambutol's effects on mycomembrane dynamics, we examined ethambutol-treated cells by FRAP analysis, which revealed increased fraction of mobile glycolipids in a drug-dose-dependent manner (Figure 6 C,D and Figure S11). Our results demonstrate that mycomembrane fluidity can be altered with sublethal antibiotic concentrations, which could improve permeability and drug accessibility in the context of co-therapy. Modulation of mycomembrane integrity with sublethal concentrations of ethambutol has been previously shown to reverse *Mtb* resistance to clarithromycin,[43] suggesting reduction of the barrier effectiveness of the mycomembrane. Moreover, increased susceptibility to the β-lactam cefepime has been observed during co-treatment with ethambutol.[44] Together, these reports provide precedent for potentiating approved therapeutics and repurposing high MIC drugs by co-treatment with low concentrations of ethambutol.[6] Understanding how the permeability of the bacterial cell envelope can be modulated could facilitate the design or access of new therapeutic agents.

CONCLUSION

The complex and unusual cell envelope of mycobacteria has captured the attention of biologists, chemists, and biophysicists alike for almost a century. Tightly packed mycolic acids in the mycomembrane were first predicted by Minnikin to explain the observed impermeability to lipophilic molecules.[24,45] Nikaido and co-workers validated the prediction of a quasi-crystalline arrangement of mycolic acids extending perpendicularly from the cell wall plane by X-ray absorption studies.[46] As well, they elegantly studied the mobility of spin-labeled fatty acids inserted into mycomembranes from *M. chelonae* cell walls.[47] Additionally, DSC studies provided an empirical foundation for our understanding of membrane fluidity in terms of phase transition temperatures across bacterial cell walls.[25] This pioneering series of studies provided insights into mycomembrane dynamics in the context of isolated cell wall preparations but could not be extended to studies in live cells.

The targeted metabolic labeling strategy used herein enabled direct interrogation of trehalose glycolipids in live cells, in their native context, with minimal perturbation. With this approach, we quantitated trehalose glycolipid mobilities and found a relationship between diffusion kinetics and mycolic acid chain structure. We also discovered that ethambutol, a front-line TB drug, enhances mycomembrane fluidity at sublethal doses, an effect that may underlie its synergism with other TB drugs. Consistent with this postulate is a recent report that

mycobacteriophage SWU1 gp39 affects *M. smegmatis*' cell envelope permeability and thereby potentiates the efficacy of multiple antibiotics.[48] These observations argue that more high-throughput screens against *Mtb* should be performed in the presence of a mycomembrane-compromising agent such as ethambutol.[44,49−52]

Furthermore, the imaging method we developed here could be adapted to visualize trehalose glycolipid dynamics in the context of host cell infection, as trehalose is metabolically orthogonal to eukaryotic hosts. Consequent insights could provide avenues for development of new drug combinations for the treatment of TB.

ASSOCIATED CONTENT

⑤ Supporting Information

The Supporting Information is available free of charge on the ACS Publications website at DOI: 10.1021/jacs.6b12541.

> Experimental procedures, characterization data, supporting figures, and schemes (PDF)

AUTHOR INFORMATION

Corresponding Author

*bertozzi@stanford.edu

ORCID

Carolyn R. Bertozzi: 0000-0003-4482-2754

Notes

The authors declare no competing financial interest.

REFERENCES

(1) World Health Organization. *Global Tuberculosis Report 2015*, 20th ed.; World Health Organization: Geneva, 2015.

(2) Russell, D. G. *Nat. Rev. Mol. Cell Biol.* **2001**, 2 (8), 569.

(3) Philips, J. A.; Ernst, J. D. *Annu. Rev. Pathol.: Mech. Dis.* **2012**, 7 (1), 353.

(4) Jarlier, V.; Nikaido, H. *FEMS Microbiol. Lett.* **1994**, 123 (1), 11.

(5) Zhang, Y. *Annu. Rev. Pharmacol. Toxicol.* **2005**, 45 (1), 529.

(6) Zumla, A.; Nahid, P.; Cole, S. T. *Nat. Rev. Drug Discovery* **2013**, 12 (5), 388.

(7) Jankute, M.; Cox, J. A. G.; Harrison, J.; Besra, G. S. *Annu. Rev. Microbiol.* **2015**, 69 (1), 405.

(8) Marrakchi, H.; Lanéelle, M.-A.; Daffé, M. *Chem. Biol.* **2014**, 21 (1), 67.

(9) Hoffmann, C.; Leis, A.; Niederweis, M.; Plitzko, J. M.; Engelhardt, H. *Proc. Natl. Acad. Sci. U. S. A.* **2008**, 105 (10), 3963.

(10) Zuber, B.; Chami, M.; Houssin, C.; Dubochet, J.; Griffiths, G.; Daffé, M. *J. Bacteriol.* **2008**, 190 (16), 5672.

(11) Siegrist, M. S.; Swarts, B. M.; Fox, D. M.; Lim, S. A.; Bertozzi, C. R. *FEMS Microbiol. Rev.* **2015**, 39 (2), 184.

(12) Christensen, H.; Garton, N. J.; Horobin, R. W.; Minnikin, D. E.; Barer, M. R. *Mol. Microbiol.* **1999**, *31* (5), 1561.

(13) Maloney, E. A.; Lun, S.; Stankowska, D.; Guo, H.; Rajagoapalan, M.; Bishai, W.; Madiraju, M. V. *Front. Microbiol.* **2011**, *2*, 19.

(14) Backus, K. M.; Boshoff, H. I.; Barry, C. S.; Boutureira, O.; Patel, M. K.; D'Hooge, F.; Lee, S. S.; Via, L. E.; Tahlan, K.; Barry, C. E.; Davis, B. G. *Nat. Chem. Biol.* **2011**, *7* (4), 228.

(15) Swarts, B. M.; Holsclaw, C. M.; Jewett, J. C.; Alber, M.; Fox, D. M.; Siegrist, M. S.; Leary, J. A.; Kalscheuer, R.; Bertozzi, C. R. *J. Am. Chem. Soc.* **2012**, *134* (39), 16123.

(16) Urbanek, B. L.; Wing, D. C.; Haislop, K. S.; Hamel, C. J.; Kalscheuer, R.; Woodruff, P. J.; Swarts, B. M. *ChemBioChem* **2014**, *15* (14), 2066.

(17) Foley, H. N.; Stewart, J. A.; Kavunja, H. W.; Rundell, S. R.; Swarts, B. M. *Angew. Chem., Int. Ed.* **2016**, *55* (6), 2053.

(18) Dover, L. G.; Cerdeño-Tárraga, A. M.; Pallen, M. J.; Parkhill, J.; Besra, G. S. *FEMS Microbiol. Rev.* **2004**, *28* (2), 225.

(19) Carel, C.; Nukdee, K.; Cantaloube, S.; Bonne, M.; Diagne, C. T.; Laval, F.; Daffé, M.; Zerbib, D. *PLoS One* **2014**, *9* (5), e97148.

(20) Meniche, X.; Otten, R.; Siegrist, M. S.; Baer, C. E.; Murphy, K. C.; Bertozzi, C. R.; Sassetti, C. M. *Proc. Natl. Acad. Sci. U. S. A.* **2014**, *111* (31), E3243.

(21) Favrot, L.; Grzegorzewicz, A. E.; Lajiness, D. H.; Marvin, R. K.; Boucau, J.; Isailovic, D.; Jackson, M.; Ronning, D. R. *Nat. Commun.* **2013**, *4*, 2748.

(22) Favrot, L.; Lajiness, D. H.; Ronning, D. R. *J. Biol. Chem.* **2014**, *289* (36), 25031.

(23) Kuru, E.; Hughes, H. V.; Brown, P. J.; Hall, E.; Tekkam, S.; Cava, F.; de Pedro, M. A.; Brun, Y. V.; VanNieuwenhze, M. S. *Angew. Chem., Int. Ed.* **2012**, *51* (50), 12519.

(24) Brennan, P. J.; Nikaido, H. *Annu. Rev. Biochem.* **1995**, *64* (1), 29.

(25) Liu, J.; Barry, C. E.; Besra, G. S.; Nikaido, H. *J. Biol. Chem.* **1996**, *271* (47), 29545.

(26) George, K. M.; Yuan, Y.; Sherman, D. R.; Barry, C. E. *J. Biol. Chem.* **1995**, *270* (45), 27292.

(27) Yuan, Y.; Crane, D. C.; Musser, J. M.; Sreevatsan, S.; Barry, C. E. *J. Biol. Chem.* **1997**, *272* (15), 10041.

(28) Ishikawa-Ankerhold, H. C.; Ankerhold, R.; Drummen, G. P. C. *Molecules* **2012**, *17* (12), 4047.

(29) Ghosh, A. S.; Young, K. D. *J. Bacteriol.* **2005**, *187* (6), 1913.

(30) Schindler, M.; Osborn, M. J.; Koppel, D. E. *Nature* **1980**, *285* (5762), 261.

(31) Muhlradt, P. F.; Menzel, J.; Golecki, J. R.; Speth, V. *Eur. J. Biochem.* **1973**, *35*, 471.

(32) Yang, Y.; Shi, F.; Tao, G.; Wang, X. *J. Microbiol.* **2012**, *50* (2), 235.

(33) Baba, T.; Kaneda, K.; Kusunose, E.; Kusunose, M.; Yano, I. *Lipids* **1988**, *23* (12), 1132.

(34) Nishiuchi, Y.; Baba, T.; Yano, I. *J. Microbiol. Methods* **2000**, *40* (1), 1.

(35) Nishiuchi, Y.; Baba, T.; Hotta, H. H.; Yano, I. *J. Microbiol. Methods* **1999**, *37* (2), 111.

(36) Barkan, D.; Liu, Z.; Sacchettini, J. C.; Glickman, M. S. *Chem. Biol.* **2009**, *16* (5), 499.

(37) Hett, E. C.; Rubin, E. J. *Microbiol. Mol. Biol. Rev.* **2008**, *72* (1), 126.

(38) Takayama, K.; Armstrong, E. L.; Kunugi, K. A.; Kilburn, J. O. *Antimicrob. Agents Chemother.* **1979**, *16* (2), 240.

(39) Telenti, A.; Philipp, W. J.; Sreevatsan, S.; Bernasconi, C.; Stockbauer, K. E.; Wieles, B.; Musser, J. M.; Jacobs, W. R. *Nat. Med.* **1997**, *3* (5), 567.

(40) Kilburn, J. O.; Takayama, K. *Antimicrob. Agents Chemother.* **1981**, *20* (3), 401.

(41) Mikusová, K.; Slayden, R. A.; Besra, G. S.; Brennan, P. J. *Antimicrob. Agents Chemother.* **1995**, *39* (11), 2484.

(42) Li, X.-Z.; Zhang, L.; Nikaido, H. *Antimicrob. Agents Chemother.* **2004**, *48* (7), 2415.

(43) Bosne-David, S.; Barros, V.; Verde, S. C.; Portugal, C.; David, H. L. *J. Antimicrob. Chemother.* **2000**, *46* (3), 391.

(44) Abate, G.; Hoffner, S. E. *Diagn. Microbiol. Infect. Dis.* **1997**, *28* (3), 119.

(45) Minnikin, D. E. Lipids: Complex Lipids, Their Chemistry, Biosynthesis and Roles. In *The Biology of the Mycobacteria*; Ratledge, C, Stanford, J., Eds.; Academic Press: New York, 1982; Vol. *1.44.* Physiology, Identification and Classification, p 95.

(46) Nikaido, H.; Kim, S.-H.; Rosenberg, E. Y. *Mol. Microbiol.* **1993**, *8* (6), 1025.

(47) Liu, J.; Rosenberg, E. Y.; Nikaido, H. *Proc. Natl. Acad. Sci. U. S. A.* **1995**, *92* (24), 11254.

(48) Li, Q.; Zhou, M.; Fan, X.; Yan, J.; Li, W.; Xie, J. *Sci. Rep.* **2016**, *6*, 28701.

(49) Farha, M. A.; Brown, E. D. *Ann. N. Y. Acad. Sci.* **2015**, *1354* (1), 54.

(50) Ramón-García, S.; Ng, C.; Anderson, H.; Chao, J. D.; Zheng, X.; Pfeifer, T.; Av-Gay, Y.; Roberge, M.; Thompson, C. *Antimicrob. Agents Chemother.* **2011**, *55* (8), 3861.

(51) Ramón-García, S.; González del Río, R.; Villarejo, A. S.; Sweet, G. D.; Cunningham, F.; Barros, D.; Ballell, L.; Mendoza-Losana, A.; Ferrer-Bazaga, S.; Thompson, C. *Sci. Rep.* **2016**, *6*, 34293.

(52) Rens, C.; Laval, F.; Daffé, M.; Denis, O.; Frita, R.; Baulard, A.; Wattiez, R.; Lefèvre, P.; Fontaine, V. *Antimicrob. Agents Chemother.* **2016**, *60*, 6193.